

Physical properties of pure In_2O_3 thin films

S. KALEEMULLA^{a*}, A. SIVASANKAR REDDY^b, S. UTHANNA^c, P. SREEDHARA REDDY^c

^aDepartment of Physics, Thin films laboratory, V.I.T. University, Vellore-632 014, India

^bDepartment of Ceramic Engineering, Yonsei University, Seol 120-749, Korea

^cDepartment of Physics, Sri Venkateswara University, Tirupathi, 517 502, India

Transparent conductive pure indium oxide (In_2O_3) thin films have been deposited on glass substrates by an activated reactive evaporation method and studied the effect of substrate temperature on the structural, electrical, optical and photoluminescence properties of the deposited films. The films were crystallized in cubic structure having an average optical transmittance of 80 % in visible region with low electrical resistivity of $9.7 \times 10^{-4} \Omega\text{cm}$ exhibiting an intensive photoluminescence emission peaks at 415 nm and 440 nm.

(Received November 1, 2008; accepted November 27, 2008)

Keywords: Indium oxide, Activated reactive evaporation, Transparent conducting oxide

1. Introduction

In recent years, thin films have become an intrinsic part of every day life and much interest has been shown in the use of transparent semiconducting oxides; as light interact with electronically active materials. Transparent conducting oxides (TCOs) are the materials, which exhibit high optical transparency in visible region (>80%) with low electrical resistivity ($\rho < 10^{-3} \Omega\text{cm}$) and high reflectivity in infrared region of the electromagnetic spectrum [1-3]. Transparent conductors have found major applications in number of microelectronic and optoelectronic devices such as heat reflecting mirrors for glass windows [4], biological systems [5], solar cells [6], flat panel displays [7], light emitting diodes [8], photodiodes [9] and heat reflecting mirrors for air craft and car windows [10]. TCOs such as SnO_2 , ZnO and CdO has been studied extensively by many researchers as they exhibit a combination of optical, electrical, mechanical and chemical properties which suggest a vast technological and economical potential. Among these oxide materials, In_2O_3 is one of the best TCO as it is n-type degenerate transparent semiconducting oxide which has a complex (cubic bixbyite Mn_2O_3 (I)) structure originating from an array of an undoped tetrahedral oxygen anion sites with wide band gap of 3.5 eV. A variety of deposition techniques such as vacuum evaporation [10], reactive thermal evaporation [11], electron beam evaporation [12], sputtering [13], spray pyrolysis [14] and activated reactive evaporation [15], etc. were applied for the preparation of TCO films with high transmittance and high conductivity.

In_2O_3 is an insulator in its stoichiometric form, but in its oxygen deficient form (InO_x), it acquires high n-type doping levels as a result of intrinsic defects, namely oxygen vacancies. Thus a variety of electrical properties can be obtained (metallic, semi conducting or insulating) depending on the stoichiometry without any impurity doping. Hence the creation of oxygen vacancies

contributes significant conduction electrons responsible for low resistivity in undoped In_2O_3 films. The high content oxygen vacancies creates an impurity band that overlaps the lower part of the conduction band resulting in a degenerate semiconductor.

2. Experimental

Thin films of In_2O_3 were prepared by using a home built activated reactive evaporation system [15] which is extensively used to deposit highly adherent films of oxides and carbides (SnO_2 , In_2O_3 , TiC etc) at lower substrate temperatures. Thin films of In_2O_3 were prepared in 12" vacuum coating unit (Model: 12A4D) consisted of a resistively heated source in which the source to substrate distance could be varied to 120 mm. The vacuum chamber was pumped to a base pressure of 3×10^{-6} mbar using diffusion pump backed by the rotary pump and the pressure in the chamber was measured using digital pirani and penning gauges, respectively. The high purity oxygen (99.999%) was admitted into the chamber through a needle valve. The flow of oxygen was controlled by Tylan mass flow controllers (Model: FC-206). The glass substrates were cleaned ultrasonically by standard means and were mounted over a plat form fixed with a resistive heater assembly capable of raising the substrate temperature up to 773 K. A chromel-alumel thermocouple was placed over the substrate surface to monitor the temperature. A dc power supply with a current range of 1A at 1000 V was used as the power source. Thin films were prepared on well cleaned glass substrates maintained in the temperature range 303 K to 573 K. The high density plasma enhances the reactivity between ionized oxygen species and indium vapors. Ultimately, the reacted vapors condense onto substrate surface. The deposition parameters of the films are tabulated in Table 1.

Table 1. Deposition parameters during the preparation of In₂O₃ films.

Source material	99.999% pure Indium metal specs
Substrates	Corning 7059 glass (75 mmx25 mmx1 mm)
Source to substrate distance	150 mm
Base pressure in the chamber	3×10^{-6} mbar
Oxygen partial pressure (PO ₂)	2×10^{-3} mbar
Substrate temperature (T _s)	303-573 K

In the present study, the structural, morphological, optical, and photoluminescence (PL) properties of the films were characterized by Seifert X-ray diffractometer (Cu k_{α} = 1.5406 Å), scanning electron microscope (JSM-840A), Hitachi U-3400 UV-VIS-NIR double beam spectrophotometer and SPEX Florolog-3 flash lamp, respectively. The electrical resistivity and Hall measurements were carried out using standard van der Pauw technique.

3. Results and discussion

3.1 Structural properties of In₂O₃ films

The as grown films were highly adherent, uniform and pin hole free. Fig. 1 shows the X-ray diffraction patterns of the as deposited indium oxide films prepared at various substrate temperatures in the range of 303 K to 573 K. The films deposited at room temperature are amorphous in nature which may be due to lower mobility of ad-atoms, which decreases the probabilities of interactions among the deposited molecules. The crystallinity of the films started to increase at the substrate temperature of 373 K which may be due to high density plasma used in this study and substrate temperature applied to the substrates which caused to initiate the crystallization in the films. The films are in polycrystalline nature with cubic structure. The diffraction peaks were observed at $2\theta = 30.5^{\circ}$ (222) and $2\theta = 36.5^{\circ}$ (400). The intensity of the diffracted peaks increased with the increase of substrate temperature from 373 K to 573 K.

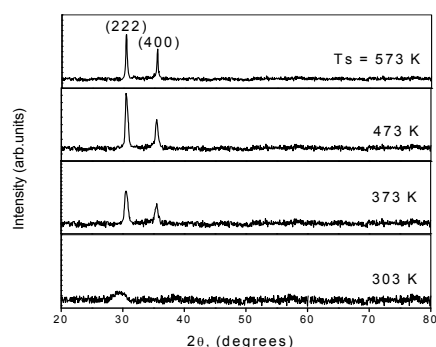


Fig.1. X-ray diffraction patterns of In₂O₃ films prepared at different substrate temperatures.

The mean crystallite size, L was calculated by using Scherrer's equation [16],

$$L = k\lambda / \beta \cos\theta \quad (1)$$

Where, λ is the wavelength of the X-rays, β is the full width at half maximum (FWHM) and θ is the Bragg's diffraction angle. The crystallite size of the films increased from 33 nm to 45 nm and lattice constant of the films decreased from 10.16 Å to 10.12 Å with the increase of substrate temperature from 373 K to 573 K as shown in Fig. 2 and these values are correlating with the previously reported values [17]. Bender et al [18] had observed a decrease of lattice constant in sputter deposited In₂O₃ films from 10.32 Å to 10.28 Å when the temperature increased from room temperature to 573 K. But no significant effect of substrate temperature on the lattice constant was observed in vacuum evaporated In₂O₃ films by Gopchandran et al [19]. One of the possible reasons for the shrinkage of lattice parameter with substrate temperature may be due to the compressive stresses developed in the films.

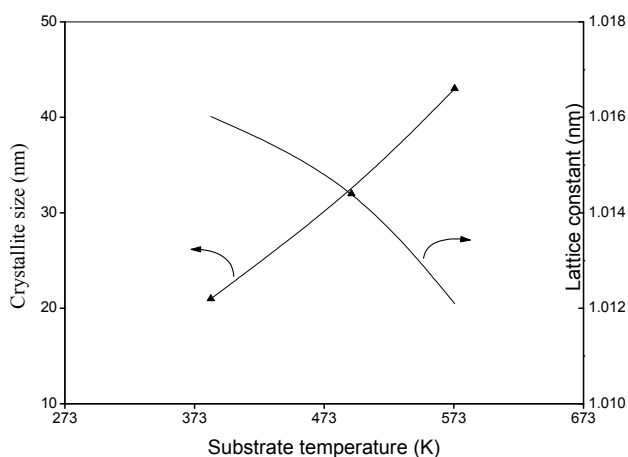
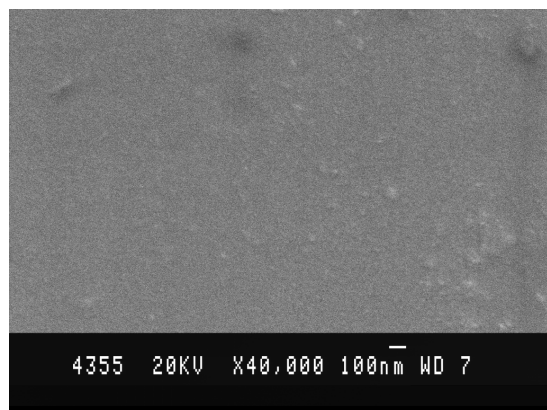


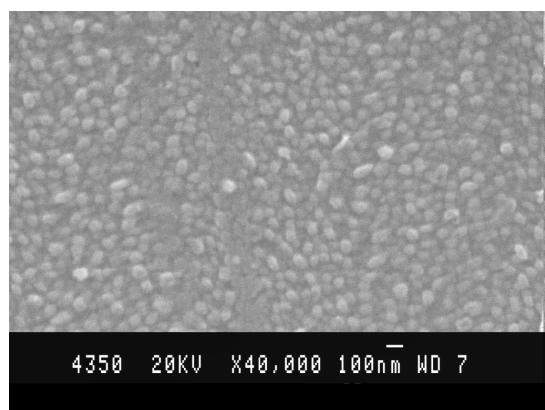
Fig. 2. Variation of crystallite size and lattice parameter with substrate temperature.

3.2 Surface analysis of In₂O₃ films

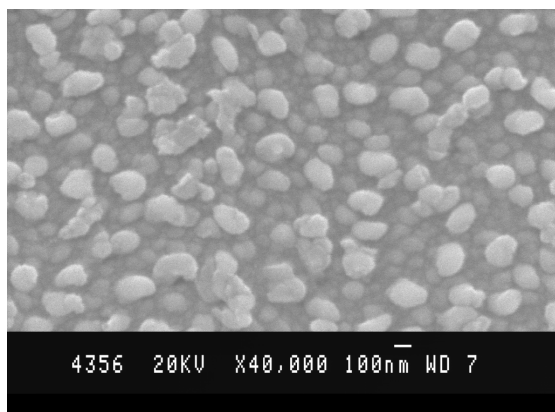
Fig. 3 (a), (b) and (c) show the surface morphology of the films deposited at different substrate temperatures. The scanning electron micrographs (SEM) were used to examine the surface morphology of indium oxide thin films. From the SEM images, it is found that the grain size of the films is highly influenced by the substrate temperature. The grain size of the films increased with increase of substrate temperature. As the substrate temperature increased, more number of atoms diffused over the substrate to form clusters. The measured mean grain size is 40 nm (573 K), a value, which is close to the mean crystallite size obtained from the XRD data.



(a)



(b)



(c)

Fig. 3. Scanning electron micrographs images of In_2O_3 films formed at different substrate temperatures (a) 303 K, (b) 473 K and (c) 573 K.

3.3 Optical properties of In_2O_3 films

Fig. 4 shows the optical transmittance spectra of the In_2O_3 films deposited at different substrate temperatures. The films showed an average transmittance of above 80 % at 600 nm and transmittance was found to be sensitive to the substrate temperature. The films show the low optical transmittance of 55 % at the low substrate temperature of 303 K.

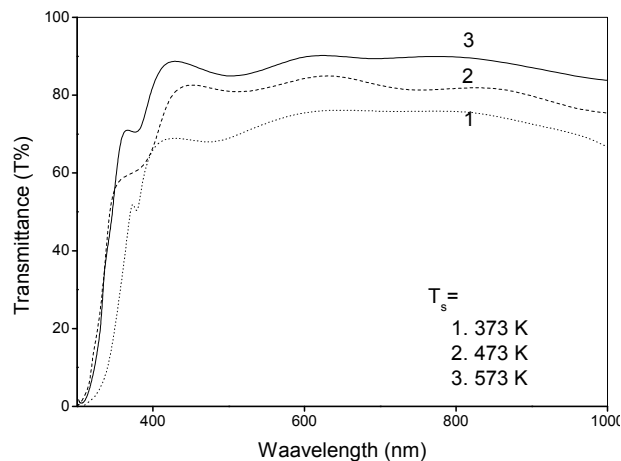


Fig. 4. Optical transmittance spectra of In_2O_3 films prepared at different substrate temperatures.

The low optical transmittance at lower substrate temperature was due to high surface light scattering of the films, which may cause of poor crystallinity of the films. When substrate temperature increased from 373 K to 573 K, the transmittance of the films increased from 75 % to 85 % which may be due to increase in crystallinity, uniformity and complete oxidation of indium with substrate temperature. The optical absorption coefficient was determined by using the relation

$$\alpha = -\ln(T) / t \quad (2)$$

where, T is the transmittance and t is the thickness of the films. It was in the range $(1.5 - 0.65) \times 10^4 \text{ cm}^{-1}$. Thickness of the film was calculated using the Manificier's relation [20] and the thickness of the films was in the range of 200 – 250 nm. The absorption edge of the films shifted towards shorter wavelength with increasing substrate temperature from 373 K to 573 K suggesting a widening of the energy band gap that could be called as Burstein-Moss shift [21]. The shift occurs owing to blocking of lowest conduction band state by partial filling of electrons. The dependence of α with the photon energy ($h\nu$) was found to obey the following relation

$$\alpha h\nu = A (h\nu - E_g)^{1/2} \quad (3)$$

where, A is a constant and E_g is the optical band gap. The value of optical band gap (E_g) can be obtained by extrapolation of the linear region of the plots to zero absorption ($\alpha = 0$). The variation of optical band gap of the films at different substrates is shown in Fig. 5. The optical band gap of the films increased from 3.41 eV to 3.48 eV with increase of substrate temperature from 373 K to 573 K. Similar behavior was observed in dc magnetron sputtered CdO films [22] in which optical band gap of the films increased from 2.41 eV to 2.53 eV with the increase of substrate temperature from 348 K to 723 K.

3.4 Electrical properties of In₂O₃ films

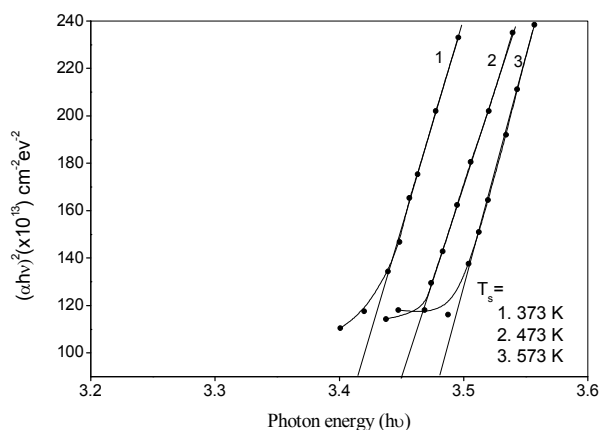


Fig. 5. Plots of $(\alpha hv)^2$ Vs $h\nu$ of the In_2O_3 films for different substrate temperatures.

Fig. 6 shows the effect of substrate temperature on the electrical resistivity and carrier concentration of pure In₂O₃ films. Generally conduction electrons in the transparent conducting oxide films are supplied from native donors such as oxygen vacancies and doping concentration. Since In₂O₃ is n-type degenerate semiconductor, the electrical properties of pure In₂O₃ is known to rely entirely on the oxidation state of the constituent i.e. either oxygen vacancies or interstitial indium atoms are expected to be donors in pure In₂O₃. The resistivity of the films decreased from $2.3 \times 10^{-3} \Omega \text{cm}$ to $9.7 \times 10^{-4} \Omega \text{cm}$ with the increase of substrate temperature from 373 K to 573 K. The decrease in resistivity caused by the increase in carrier concentration, which varied from $9.9 \times 10^{19} \text{cm}^{-3}$ to $2.2 \times 10^{20} \text{cm}^{-3}$ with the increase of substrate temperature from 373 K to 573 K. The electrical resistivity and optical transmittance of pure, Sn and Mo doped In₂O₃ films are tabulated in Table 2.

Table 2. Summary of electrical resistivity and optical transmittance of pure and doped In₂O₃ films.

Sample	Substrate temperature (T _s)	Resistivity (Ωcm)	Transmittance (T%)	Reference
IMO	723	7.3×10^{-4}	90	[23]
IMO	623	4.8×10^{-4}	87	[24]
ITO	773	3.3×10^{-4}	90	[25]
ITO	673	5.0×10^{-4}	80	[26]
Pure In ₂ O ₃	473	7.9×10^{-4}	74	[27]
Pure In ₂ O ₃	573	9.7×10^{-4}	85	Present work

$$\Phi_{TC} = T^{10} / \rho_s \quad (4)$$

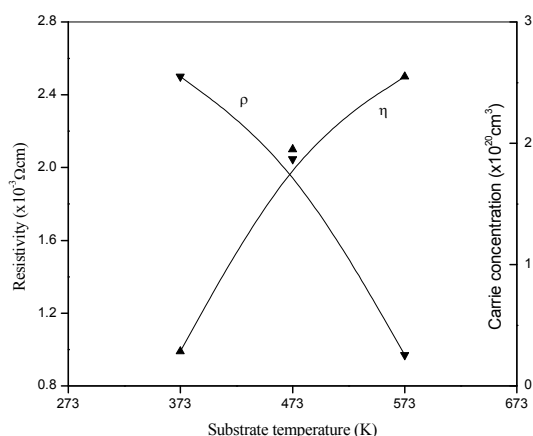


Fig.6. Variation of electrical resistivity and carrier concentration as a function of substrate temperature

The performance of transparent conducting oxides can be measured using Haacke's figure of merit relation [28],

where, T is the transmittance at 600 nm and ρ_s is the sheet resistance of the films. Fig. 7 shows the variation of figure of merit (Φ_{TC}) with different substrate temperatures. The figure of merit increased from $0.61 \times 10^{-3} \Omega^{-1}$ to $5.18 \times 10^{-3} \Omega^{-1}$ with the increase of substrate temperature from 373 K to 573 K. The increase of figure of merit with substrate temperature was due to the decrease in the electrical resistivity as well as increase in optical transmittance. Higher is the figure of merit, better is the performance of the transparent conducting film. Figure of merit of the films for different substrate temperatures is tabulated in Table 3. The best performance of the samples was obtained at a substrate temperature of 573 K with $\Phi_{TC} = 5.32 \times 10^{-3} \Omega^{-1}$.

Table 3. Summary sheet resistance and transmittance of In₂O₃ films.

Substrate temperature (T _s)	Sheet resistance (ρ_s)	Transmittance (T%)	Figure of merit (Φ_{TC}) ($\times 10^{-3} \Omega^{-1}$)
373	92	75	0.61
473	60	81	2.01
573	37	85	5.32

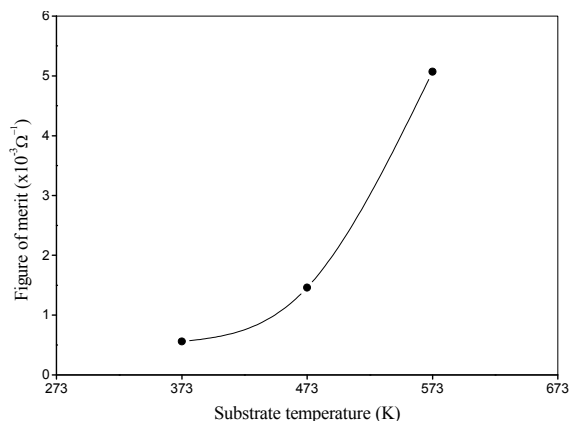


Fig. 7. Variation of figure merit of In_2O_3 films with substrate temperature.

3.5 Photoluminescence properties of In_2O_3 films

Fig. 8 shows the emission photoluminescence spectra of pure indium oxide thin films formed on glass substrates. Photoluminescence emission peaks were observed which could be seen by the naked eye. Two distinct peaks in the PL spectrum were shown in blue region at 415 nm and 440 nm wavelength under the excitation of 375 nm at room temperature. It is well known that bulk In_2O_3 cannot emit light at room temperature [29]. But here when the films were characterized at room temperature showed the PL emission peaks and the intensity of the PL peaks increased with the increase of substrate temperature. The origin of the PL may be due to the defects or oxygen deficiencies formed in the films structures. The intensive blue region can be attributed to oxygen vacancies and indium-oxygen vacancy centers $(\text{VIn}, \text{VO})^X$ may be acted as the acceptors and VO^X as the donors. After excitation of the acceptor, a hole on the acceptor and an electron on a donor are created according to the equation

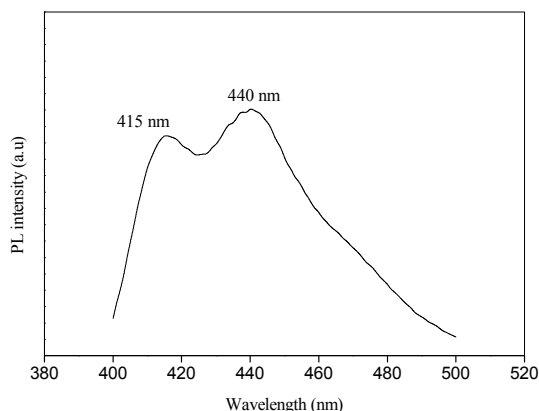
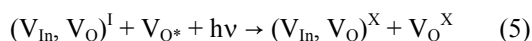


Fig. 8. Photoluminescence spectra (PL) of the In_2O_3 films at room temperature formed on glass substrate.

Luminescence process can be explained in two steps. At first, an electron in donor level (VO^X) may be captured by a hole on an acceptor $[(\text{VIn}, \text{VO})^X]$ to form a trapped exciton and in the next step the trapped exciton recombines radiatively to produce the observed blue emission. In the previous studies strong peaks in the PL spectrum were observed at 637 nm, 470 nm and 1540 nm in thermal oxidation of indium films [30], single crystalline In_2O_3 films [31] and erbium doped In_2O_3 films [32], respectively. Further investigation is required for the exact origin of Photoluminescence. One of the possible reasons is explained as follows. When the indium oxide films were prepared at high temperature, oxygen vacancies and oxygen-indium vacancy pairs might have been produced. Therefore, it seem that the intense blue light emission can be attributed to oxygen vacancies and indium-oxygen vacancy centers.

4. Conclusions

From the XRD studies it is found that the In_2O_3 films were cubic in structure and predominantly oriented along (222) plane. The SEM investigations showed that the grain size of the films increased with the increase of substrate temperature from 373 K to 573 K. Optical band gap E_g of the films varied from 3.41 eV to 3.48 eV for the films deposited at different substrate temperatures. The lowest resistivity of $9.7 \times 10^{-4} \Omega \text{cm}$ with a figure of merit $5.32 \times 10^{-3} \Omega^{-1}$ was obtained for the films deposited at 573 K. The intense blue PL bands at 415 and 440 nm have been observed. These characteristics of the pure indium oxide films may have potential applications in electro-optical devices as a blue light source.

References

- [1] R. Bel, H. Tahar, T. Ban, Y. Ohaya, Y. Takahashi, J. Appl. Phys., **82**, 865 (1997).
- [2] M. H. Sohan, D. Kim, S. J. Kim, N. W. Paik, J. Vac. Sci. Technol. A., **21**, 1347 (2003).
- [3] J. S. Cho, K. H. Yoon, S. K. Koh, J. Appl. Phys., **89**, 3223 (2001).
- [4] K. L. Chopra, S. R. Das, Thin Film Solar Cell, Plenum Press, New York, **321**, (1983).
- [5] L. Tamisier, A. Carani, Electrochem. Acta., **32**, 1365 (1987).
- [6] G. Frank, E. Kauer, H. Kostlin, Sol. Energy. Mat. **8**, 387 (1983).
- [7] J. E. Costellamo, Hand book of Display Technology, Academic Press, New York, (1992).
- [8] T. B. Hur, I. J. Lee, H. L. Park, Y. H. Hwang, H. K. Kim, Solidi State Commun. **130**, 397 (2004).
- [9] N. Biyikli, T. Kartoglu, O. Aytur, I. Kimukin, E. Ozbay, Appl. Phys. Lett., **79**, 2838 (2001).
- [10] S. Muranaka, Thin Solid Films, **221**, 1 (1992).
- [11] A. Salehi, Thin Solid Films, **324**, 214 (1998).
- [12] H. J. Krokoszinski, R. Oesterlein, Thin Solid Films, **187**, 179 (1990).

- [13] T. K. Subramanyam, B. Srinivasula Naidu, S. Uthanna, *Appl. Surf. Sci.* **169**, 529 (2001).
- [14] K. T. Ramakrishna Reddy, H. Gopalaswamy, P. J. Reddy, R. W. Miles, *J. Cryst. Growth.*, **210**, 516 (2000).
- [15] K. Srinivasa Rao, K. V. Madhuri, S. Uthanna, O. M. Hussain, C. Julien, *Mater. Sci. Eng.*, **B 100**, 79 (2003).
- [16] B. D. Cullity, *Elements of X-ray diffraction*, 2nd Ed., Addison - Wesley, Reading, M.A., **102**, (1978).
- [17] S. Honda, A. Tsujimoto, M. Watamori, K. Oura, *J. Appl. Phys.*, **34**, 1386 (1995).
- [18] M. Bender, N. Katsarakis, E. Gagaoudakis, E. Hourdakis, E. Douloufakis, V. Cimalla and G. Kiriakidis, *J. Appl. Phys.*, **90**, 10 (2001).
- [19] K. G. Gopchandran, B. Joseph, J. T. Abraham, P. Koshy, V. K. Vaidyan, *Vacuum*, **48**, 547 (1997).
- [20] J. C. Manificier, J. P. Fillard, J. M. Bind, *Thin Solid Films*, **77**, 67 (1981).
- [21] E. Bustein, *Phys. Rev.*, **93**, 632 (1952).
- [22] T. K. Subramanyam, G. Mohan Rao, S. Uthanna, *Mater. Chem. Phys.*, **69**, 133 (2001).
- [23] D. J. Seo, S.H. Park, *Physica B*, **357**, 420 (2005).
- [24] L. Huang, X. Li, Q. Zhang, W. Miao, L. Zhang, X. Yan, *J. Vac. Sci. Technol. A*, **23**, 5 (2005).
- [25] A. E. Hichou, A. Kachouane, J. L. Bubendorff, M. Addou, J. Ebothe, M. Troyon, A. Bougrine, *Thin Solid Films*, **458**, 263 (2004).
- [26] M. A. Martinez, J. Herrero, M. T. Gutierrez, *Thin Solid Films*, **269**, 80 (1995).
- [27] S. Naseem, M. Iqbal, K. Hussain, *Sol. Energy Mater. Sol. Cell*, **31**, 155 (1993).
- [28] G. Haacke, *Ann. Rev. Mater. Sci.* **7**, 73 (1977).
- [29] Y. Ohhata, F. Shinoki, *Thin Solid Films*, **59**, 255 (1979).
- [30] M. S. Lee, W. C. Choi, E. K. Kim, C. K. Kim, S. K. Min, *Thin Solid Films*, **279**, 1(1996).
- [31] P. Guha, S. Kar, S. Chaudhuri, *Appl. Phys. Letts.*, **85**, 17 (2004).
- [32] H. K. Kim, C. C. Li, G. Nykolak, P. C. Becker, *J. Appl. Phys.*, **76**, 8209 (1994).

*Corresponding author: skaleemulla@gmail.com